pharmaceutics

Supplementary Materials: Integration of *In Silico* Strategies for Drug Repositioning towards P38α Mitogen-Activated Protein Kinase (MAPK) at the Allosteric Site

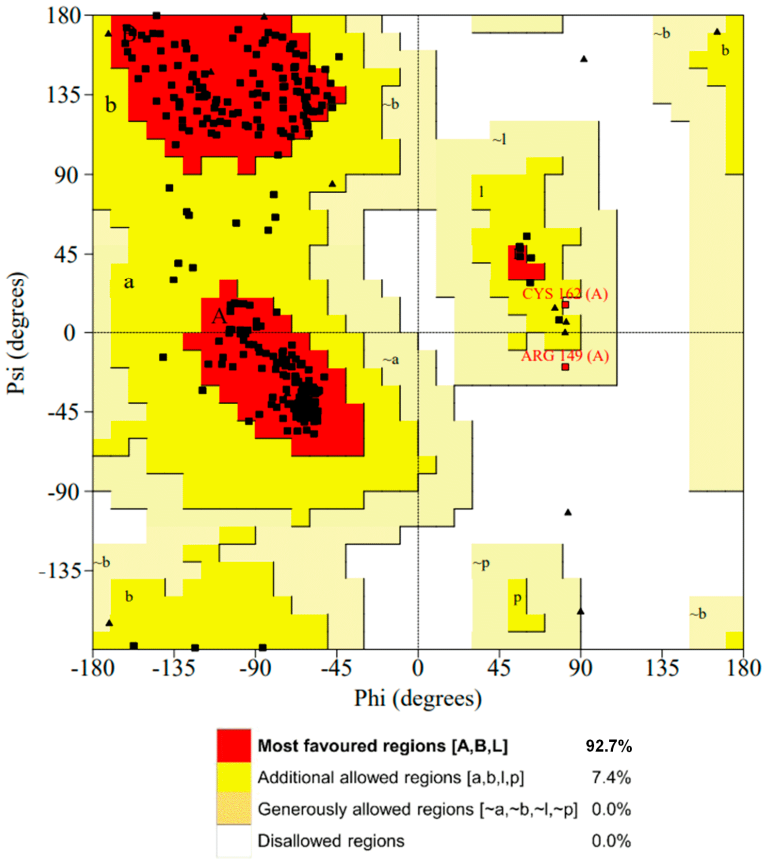

Figure S1: Ramanchandran plot analysis of a homologically constructed protein structure where the torsional conformation of amino acids was plotted. Most of them were fallen into favoured/allowed regions, which signify an acceptable quality of constructed model.

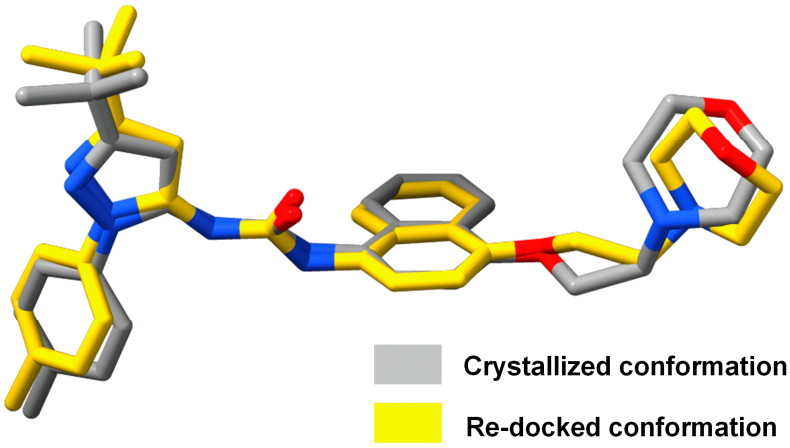

Figure S2: Alignment of the re-docked pose and available crystallized ligand (BIRB796) of p38α MAPK indicating a verified docking protocol used in this study.

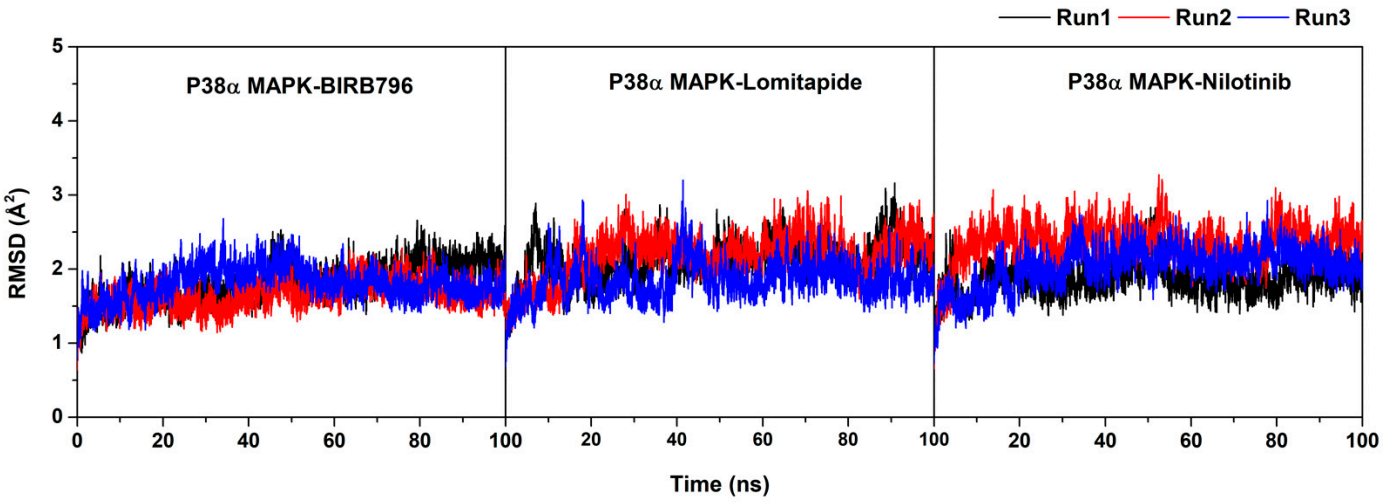

Figure S3: Plot of root-mean-square displacement (RMSD) for the backbone amino acids within 5 Å from the ligand. The data were illustrated in three independent runs with different initial velocities.

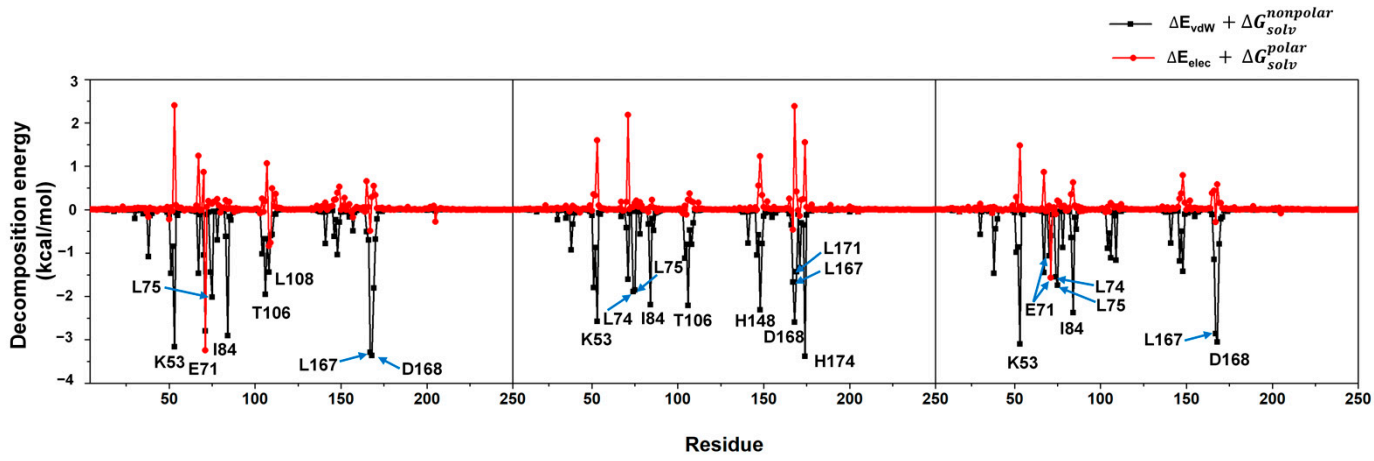

Figure S4: Analysis of per-residue VdW (ΔE_{vdW}+ $\Delta G_{sol}^{nonpolar}$) and electrostatic ($\Delta E_{ele}$+ ΔG_{sol}^{polar}) decomposition energy in which the amino acids largely contributed via VdW and electrostatic interaction energies were labeled in a one-letter code format. We noted that even though some residues (e.g.K53, H148) were noticeably stabilized through vdW interactions, they did not play a role in the binding process since they were destabilized by electrostatic charge-charge repulsion (as observed in positive electrostatic energy). Hence, these kinds of residues were not shown in the article Figure 6.

Table S1: Summary of key pharmacophore features of BIRB796, lomitapide, and nilotinib detected by using the PharmaGist web interface.

Compounds	Total Features	Aromatic moiety	Hydrophobic moiety	H-bond donor	H-bond acceptor
BIRB796	20	4	8	2	5
Lomitapide	11	4	2	2	3
Nilotinib	16	5	3	4	4

Table S2: The ΔG_{bind} value (kcal/mol) in each run and the averaged ΔG_{bind} of the two focused drug candidates and BIRB796 in complex with p38α MAPK. The calculations in three independent runs of each complex showed a similar range of ΔG_{bind} value, indicating the reproducibility of end-point SIE prediction of the binding affinity. We noted that the ΔG_{bind} listed in Table 1 were from the first run since we kept them consistent with the other eight remaining drug candidates.

Compounds	Run	Energy Components (kcal/mol)				
		E_{vdW}	E_{coul}	ΔG_{RF}	ΔG_{cavity}	ΔG_{bind}
BIRB796	1	-78.53±0.29	-9.93±0.15	15.60±0.20	-13.63±0.04	-11.95±0.04
	2	-82.37±0.28	-10.85±0.14	15.07±0.20	-13.91±0.04	-11.64±0.03
	3	-82.01±0.32	-8.32±0.16	11.41±0.19	-13.58±0.04	-11.69±0.04
			Average			**-11.76±0.04**
Lomitapide	1	-77.77±0.39	-5.95±0.18	17.01±0.24	-14.43±0.04	-11.39±0.05
	2	-78.41±0.34	-13.12±0.19	29.61±0.35	-14.58±0.06	-10.90±0.04
	3	-81.79±0.34	-6.11±0.18	16.21±0.24	-13.16±0.04	-11.78±0.04
			Average			**-11.35±0.04**
Nilotinib	1	-69.53±0.35	-13.04±0.17	15.54±0.19	-12.35±0.03	-11.21±0.04
	2	-70.47±0.37	-11.71±0.24	14.87±0.15	-12.56±0.04	-11.26±0.03
	3	-68.62±0.35	-15.35±0.21	17.51±0.18	-12.67±0.04	-11.18±0.04
			Average			**-11.21±0.04**

Table S3: The ΔG_{bind} value (kcal/mol) of the modified structure of lomitapide in complex with p38α MAPK, calculated by using end-point SIE method.

Drugs	Energy Components (kcal/mol)				
	E_{VdW}	E_{coul}	ΔG_{RF}	ΔG_{cavity}	ΔG_{bind}
Modified lomitapide	-85.37±0.46	-11.92±0.34	23.39±0.30	-14.48±0.06	-12.15±0.06